Seismicity along the Azores-Gibraltar region and global plate kinematics

M. Bezzeghoud, C. Adam, E. Buforn, J. F. Borges & B. Caldeira

Journal of Seismology

ISSN 1383-4649
Volume 18
Number 2

J Seismol (2014) 18:205-220
DOI 10.1007/s10950-013-9416-x

Springer

J Seismol (2014) 18:205–220
DOI 10.1007/s10950-013-9416-x

ORIGINAL ARTICLE

Seismicity along the Azores-Gibraltar region and global plate kinematics

M. Bezzeghoud · C. Adam · E. Buforn · J. F. Borges · B. Caldeira

Received: 11 February 2013 / Accepted: 23 December 2013 / Published online: 8 January 2014

Abstract Seismicity along the western part of the Eurasia–Nubia plate boundary displays very complex patterns. The average motion is transtensional in the Azores, dextral along the Gloria transform zone and convergent between the SW Portuguese Atlantic margin and the Ibero-Maghrebian zone. To constrain the factors controlling the seismicity, we provide a new seismotectonic synthesis using several earthquakes. We show that the study area can be divided into six different regions, with each characterised by a coherent seismicity pattern. The total seismic moment tensor and the average slip velocities are provided for each region. To determine the spatial distribution of the seismicity, we computed the slip vector for each earthquake based on its focal mechanism and compared it to the relative velocity between the Eurasian and Nubian plates, deduced from global kinematic models. Despite local departures in the Alboran Sea and near the Mid-Atlantic Ridge, we found a good correlation between these two independent vector sets. Quantitatively, the slip velocities display a linear, non-affine correlation with the norms of the relative kinematic velocities. The norms of the slip velocities also seem to depend on the tectonic regime and on the morphology of the plate boundary.

Keywords Seismicity · Global plate kinematics · Focal mechanism · Seismic slip velocity · Kinematic velocity · Slip vector · Total seismic moment tensor · Azores-Gibraltar region

M. Bezzeghoud (✉) · C. Adam · J. F. Borges · B. Caldeira
Centro de Geofísica de Évora and Physics Department, Escola de Ciências e Tecnologia (ECT), University of Évora, Évora, Portugal
e-mail: mourad@uevora.pt

E. Buforn
Departamento de Geofísica y Meteorología, Facultad CC Fisicas, Universidad Complutense, 28040 Madrid, Spain

E. Buforn
IGEO (UCM-CSIC), Facultad CC Físicas, Universidad Complutense, 28040 Madrid, Spain

1 Introduction

The western part of the Eurasia–Nubia plate boundary extends from the Azores to the Ibero-Maghrebian region. The oceanic part of the plate boundary is very well delimited from the Azores Islands, along the Azores-Gibraltar fault to approximately 12°W (west of the Strait of Gibraltar) (Fig. 1). From 12°W to 3.5°E, including the Iberia–Nubia region and extending to the western part of Algeria, the boundary is more diffuse and forms a wider area of deformation (Buforn et al. 2004; Borges et al. 2007, 2008). The boundary between the Iberia and Nubia plates is the most complex part of the margin. This region corresponds to the transition from an oceanic boundary to a continental boundary, where Iberia and Nubia collide.

Although most earthquakes along this plate boundary are shallow and generally have magnitudes of less than 5.5, there have been several high-magnitude events.

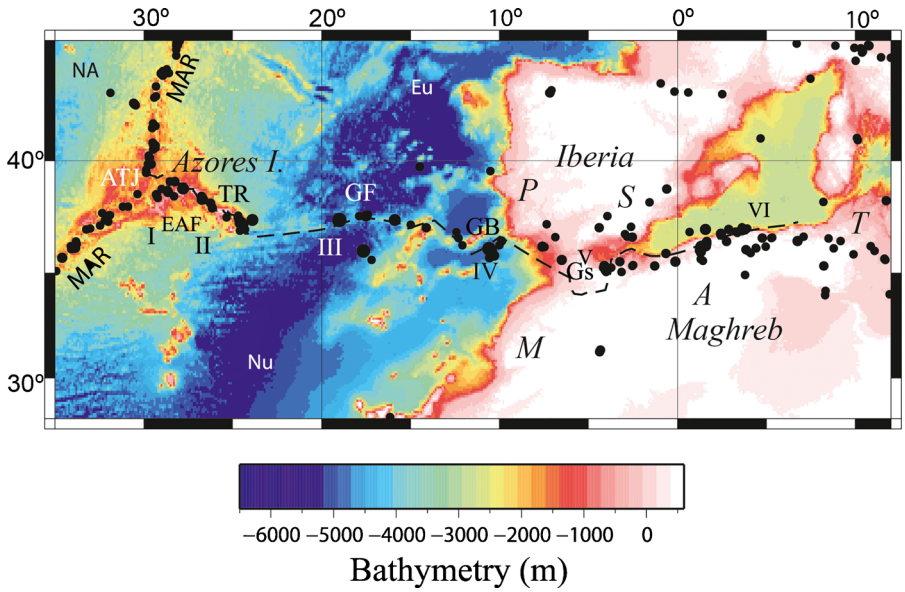

Fig. 1 Bathymetry of the study area (Smith and Sandwell 1997) and $M \geq 5.0$ seismicity along the western part of the Eurasia–Nubia plate from 1931 to 2010 (NEIC Data Files for 1973–2010 and for 1931–1972) (see Table 1). *MAR* Mid-Atlantic Ridge, *ATJ* Azores Triple Junction, *TR* Terceira Ridge, *EAF* East Azores Fracture Zone, *GF* Gloria Fault, *GB* Gorringe Bank, *Gs* Gibraltar Strait, *NA* North America plate, *Eu* Eurasia plate, *Nu* Nubia plate, *P* Portugal, *S* Spain, *A* Algeria, *M* Morocco, *T* Tunisia. The Roman numerals (*I* to *VI*) indicate the six zones studied and described in the text

From 1920 to 2010, three earthquakes with magnitudes of about 8.0 (M_w 8.2, 25 November 1941; M_s 8.0, 25 February 1969; and M_w 7.9, 26 May 1975) occurred in the oceanic region (Buforn et al. 1988), and four earthquakes with magnitudes of about 7.0 (M_w 7.1, 8 May 1939, Santa María Island and M_w 7.1, January 1980, Terceira and Graciosa Islands, both in the Azores; M_s 7.1, 20 May 1931, Azores-Gibraltar fracture zone; and Mw 7.3, 10 October 1980, El Asnam, Algeria) occurred along the western part of the Eurasia–Nubia plate boundary (Meghraoui et al. 1986; Bezzeghoud et al. 1995; Ayadi et al. 2003). In general, large earthquakes ($M \geq 7$) occur within the oceanic region, with the exception of the El Asnam (Algeria) earthquakes. Some of these events caused extensive damage.

The 1755 Lisbon earthquake (~M_w 9) on the Portugal Atlantic margin, about 200 km W–SW of Cape St. Vincent, was followed by a tsunami and fires that caused the near-total destruction of Lisbon and adjacent areas. Estimates of the death toll in Lisbon alone (10,000 and 100,000) make it one of the deadliest earthquakes in history (Machado 1966; Moreira 1985; Martínez-Solares and Lopez-Arroyo 2004). Measured in lives lost, the 1980 and 1998 Azores earthquakes (Portugal), the 1954 and 1980 El Asnam earthquakes (North Algeria), the 1994 and 2004 Alhoceima earthquakes (North Morocco), and the 2003 Boumerdes earthquakes (North Algeria) were the worst earthquakes in the past 120 years in the study area (Benouar 1994; Bezzeghoud et al. 1996; Bezzeghoud and Buforn 1999; Ayadi et al. 2003). Hence, this region has experienced many large and damaging earthquakes.

It is therefore essential to determine the factors controlling seismicity along this plate boundary to mitigate the potential damage of large earthquakes and to improve the studies of seismic risk in this area. As a first step, a better characterisation of the seismicity of this region is required. Several seismotectonic syntheses have been proposed, but they either focus on particular zones, such as the Azores (McKenzie 1972; López-Arroyo and Udías 1972; Udías et al. 1976; Borges et al. 2007, 2008) or the Ibero-Maghrebian region (Buforn et al. 2004), or they encompass the complex Western Mediterranean area (e.g. Serpelloni et al. 2007; Meghraoui and Pondrelli 2012). This study focuses on the westernmost part of the Eurasia–Nubia boundary, from the Azores to the Ibero-Maghrebian region. We have selected shallow (depth ≤40 km) $M \geq 5.0$ earthquakes (Figs. 1 and 2; Tables 1 and 2) occurring between 1931 and the present. Following Buforn et al. (2004), Borges et al. (2007) and Bezzeghoud et al. (2008), we divide the study area into six zones

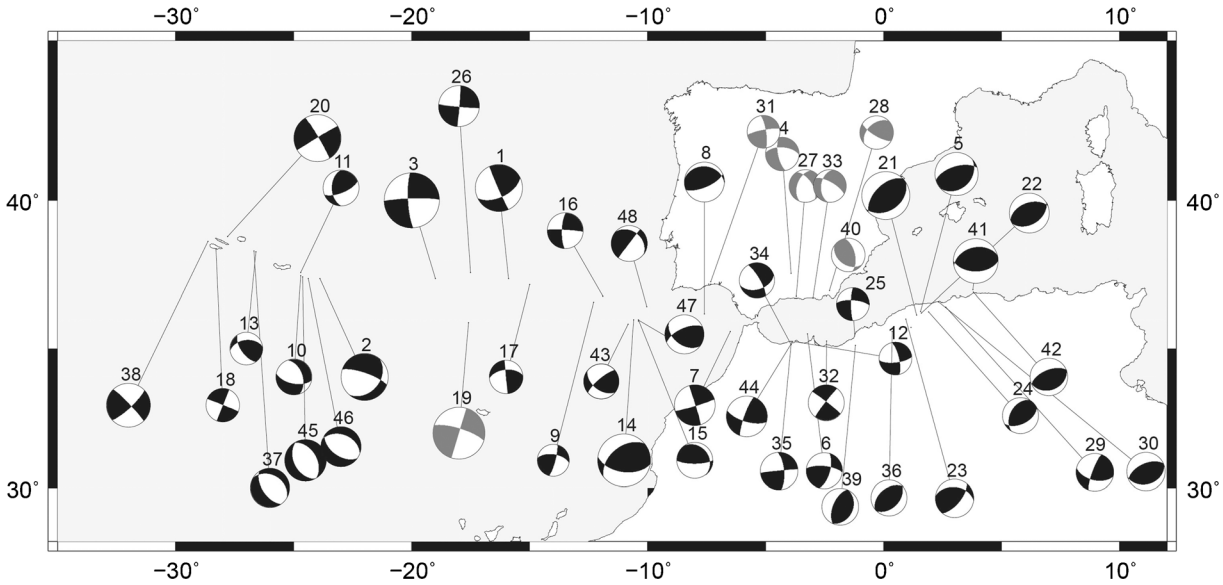

Fig. 2 Focal mechanisms for $M \geq 5.0$ shallow earthquakes (depth ≤40 km) in the western part of the Eurasia–Nubia plate boundary. Size is proportional to magnitude. Solution parameters for focal mechanisms are listed in Table 2

according to the characteristics of seismicity and focal mechanisms. For each zone, we provide the seismic moment tensor (SMT) and the average slip velocities. These six zones, numbered from I to VI, are described in Table 1 and analysed in the following sections. Table 1 summarises the more important seismotectonic characteristics for each zone from the Mid-Atlantic Ridge in the west to Algiers in the east, and it includes the location and name of the zone, the slip velocity and the predominant fault motion.

In this paper, we quantify the slip motions derived from seismicity and the focal mechanisms in this area, and we compare them with motions deduced from kinematic models. To determine the factors controlling the seismicity, we also examine how the slip vectors computed from focal mechanisms correlate with the relative kinematic velocities derived from global models. Focal mechanisms and plate kinematic models derived from geodetic space techniques like VLBI, SLR and GPS are two independent kinematic indicators that provide

Table 1 Characteristics of the western part of the Eurasia–Nubia plate boundary, from the Mid-Atlantic Ridge in the west to Algiers in the east. The six zones are located and identified, and the corresponding predominant motion is described for each zone by the slip velocity. More details are given in the text and illustrated in Fig. 3. D2k and Nu1A represent, respectively, DEOS2k and Nuvel 1-A. DEOS2k is a model for the current motion of seven major tectonic plates derived from space-geodetic observations and is based on ITRF2000 (Altamimi et al. 2002) and African GPS observations (Fernandes et al. 2003). Nuvel-1A model (DeMets et al. 1990) is described in the text

Zone	Left lat. to right lat.	Name of the zone	Slip velocity (mm/year)	Nu1A (mm/year)	D2k (mm/year)	Predominant motion
I	30°W to 27°W	Triple junction to Terceira Island	6.7	4.5	4.2	Left-lateral strike-slip faulting, with horizontal pressure
II	27°W to 23°W	Azores Islands	3.1			Normal faulting, with horizontal tension axis trending to NE–SW
III	23°W to 11°W	Gloria Fault	18	2.3	–	Right-lateral transform fault
IV	11°W to 6°W	Gorringe Bank to Cadiz	5.5	4.3	5.0	Thrust
V	6°W to 1°W	Betic, Rif Cordilleras and Alboran Sea	1.4	5.2	5.3	Complex pattern: strike-slip and normal
VI	1°W to 3.5°E	NW Algeria and Tell Mountains	3.7	5.6	5.4	Thrust

Table 2 Source parameters of $M \geq 5.0$ shallow earthquakes (depth ≤40 km) for the western part of the Eurasia–Nubia plate boundary from 1931 to 2010 (see Fig. 1). M_w, M_s and M represent, respectively, moment, surface wave and unified magnitude

Date	Lat.N.	Long.E	h (km)	M	ϕ	δ	λ	NF	Ref
20 May 1931	37.4	−15.9	15	M 7.1	64	59	4	1	B88
08 May 1939	37.40	−23.90	15	M 7.1	41	35	−154	2	B88
25 Nov. 1941	37.40	−19.00	15	M 8.4	177	79	−6	3	B88
19 May 1951	37.58	−3.93	30	M 5.1	169	69	−35	4	B04
09 Sept. 1954	36.28	1.57	10	M 6.5	253	61	104	5	B99
23 Aug. 1959	35.51	−3.23	20	M 5.5	276	70	153	6	B99
05 Dec. 1960	35.60	−6.50	15	M_s 6.2	73	86	−178	7	B88
15 March 1964	36.20	−7.60	12	M_s 6.1	276	24	117	8	B88
29 June 1965	36.6	−12.3	15	M 5.0	15	80	32	9	B88
04 July 1966	37.50	−24.70	10	M 5.4	341	49	−42	10	B88
05 July 1966	37.60	−24.70	18	M 5.1	179	48	30	11	B88
17 April 1968	35.24	−3.73	22	M 5.0	83	70	−162	12	B99
20 April 1968	38.30	−26.60	15	M 5.0	264	45	39	13	B88
28 Feb. 1969	36.10	−10.60	22	M_w 7.8	231	47	54	14	B95
05 May 1969	36.00	−10.40	29	M_s 5.5	324	24	142	15	B95
06 Sept. 1969	36.90	−11.90	35	M_s 5.5	182	75	−5	16	B88
30 Dec. 1970	37.20	−15.00	15	M_s 5.1	265	54	1	17	B88
23 Nov. 1973	38.40	−28.30	15	M_s 5.1	292	89	−0	18	B88
26 May 1975	35.90	−17.60	15	M_s 7.9	287	76	180	19	G86
01 Jan. 1980	38.80	−27.80	10	M_w 6.9	239	88	−5	20	B99
10 Oct. 1980	36.16	1.39	5	M_w 7.3	225	54	83	21	B99
10 Oct. 1980	36.24	1.59	10	M_w 6.1	58	43	81	22	B99
07 Dec. 1980	36.02	0.94	5	M_w 5.8	277	40	140	23	B99
01 Feb. 1981	36.27	1.90	11	M_w 5.5	210	43	64	24	B99
15 Nov. 1992	35.73	1.15	7	M_w 5.0	274	70	−169	25	CMT
17 Oct. 1983	37.60	−17.50	4	M_s 6.0	95	88	−178	26	B88
24 June 1984	36.80	−3.70	5	M_w 5.0	201	48	−46	27	B99
13 Sept. 1984	37.00	−2.30	9	M_w 5.1	121	73	156	28	B99
31 Oct. 1988	36.44	2.63	13	M_w 5.7	103	55	167	29	B99
29 Oct. 1989	36.61	2.33	31	M_w 5.8	242	55	87	30	B99
20 Dec. 1989	37.30	−7.30	23	M_w 5.0	351	77	10	31	B95
23 April 1993	35.27	−2.42	6	M_w 5.4	308	86	4	32	B99
23 Dec. 1993	36.77	−2.99	8	M_w 5.4	300	70	−130	33	B99
26 April 1994	35.14	−3.92	7	M_w 5.3	330	77	45	34	B99
26 April 1994	35.16	−3.92	8	M_w 5.7	355	79	2	35	B99
18 Aug. 1994	35.60	0.36	4	M_w 5.7	58	45	95	36	B99
27 June 1997	38.33	−26.68	7	M_w 5.9	301	35	−111	37	B07
09 July 1998	38.65	−28.63	8	M_w 6.2	156	88	0	38	B07
22 Dec. 1999	35.34	−1.45	6	M_w 5.6	25	31	92	39	Y04
02 Feb. 1999	38.10	−1.50	1	M_w 5.1	125	39	56	40	B01
21 May 2003	37.02	3.77	6	M_w 6.8	250	40	80	41	CMT
27 May 2003	36.94	3.72	15	M_w 5.7	70	31	92	42	CMT
29 July 2003	35.80	−10.6	30	M_w 5.3	128	50	162	43	PRO

Table 2 (continued)

Date	Lat.N.	Long.E	*h* (km)	*M*	ϕ	δ	λ	NF	Ref
24 Feb. 2004	35.14	−4.00	6	M_w 6.2	305	88	179	44	CMT

ϕ azimuth, δ plunge, λ rake, *NF* number on Fig. 2, *B88* Buforn et al. (1988), *B99* Bezzeghoud and Buforn (1999), *B95* Buforn et al. (1995), *B01* Borges et al. (2001), *B07* Borges et al. (2007), *PRO* Pro et al. (2012), *Y04* Yelles-Chaouch et al. (2004), *G86* Grimison and Cheng (1986), *CMT* Centroid Moment Tensor (Harvard)

information on the ongoing crustal deformation. This approach has been used by Serpelloni et al. (2007), although they used the P and T axes to describe the motion produced by an earthquake. However, the slip vectors are more representative of the motion along a fault and are therefore more directly connected to the relative kinematic velocities. Such a correlation has, to our knowledge, not yet been investigated. The kinematic data used by Serpelloni et al. (2007) are very accurate because they integrate continuous GPS observations and data acquired during campaigns at temporary geodetic stations in regional, subregional and local networks around the Eurasia–Nubia plate boundary. In our study area, the resultant model displays directions very similar to those provided by global kinematic models. Moreover, our seismic data were determined through a more careful analysis of individual events. Finally, for a more quantitative study, we compared the norm of the relative kinematic velocities with slip velocities deduced from the seismicity.

2 Tectonics and seismicity of the study area

The Eurasia–Nubia plate boundary presents different tectonic characteristics along the margin. The Azores plateau in the west is a region of elevated topography, and it encompasses the area where three major tectonic plates (Eurasia—Eu, Nubia—Nu and North America—NA; Fig. 1) meet to form the Azores Triple Junction. The eastern side of the plateau, where our study is focused, has an approximately triangular shape. It is delimited by three major tectonic discontinuities: the Mid-Atlantic Ridge (MAR) to the west, the Terceira Ridge (TR) to the north and the East Azores Fracture (EAF) to the south, bounding the western part of the Gloria Fault (GF) (Buforn et al. 1988). This area contains numerous seamounts and seven of the Azores islands. The origin of the TR is still under debate; it may be an extensional zone normal to the MAR (e.g. Udías 1980; Buforn et al. 1988) or an oblique extension (e.g. Searle 1980). Madeira and Ribeiro (1980) propose a leaky transform model, whereas Lourenço et al. (1998) propose a diffuse boundary. Vogt and Jung (2004) suggest that this may be the slowest spreading boundary in the world.

The high level of seismicity along the MAR and the TR is associated with seafloor spreading. The moderate- and shallow-depth (≤40 km) seismicity of the Azores region is associated with the boundary between the Eu, Nu and NA plates (Fig. 1). Most of the seismic activity is located on the MAR and on the TR, whereas the EAF zone is practically inactive (Fig. 1). The seismicity follows the same trend as the islands: approximately ENE from the MAR to Terceira Island (zone I, from 30°W to 27°W) and SE from Terceira Island to San Miguel Island (zone II, from 27°W–23°W, Borges et al. 2007, 2008). The seismicity stops at 24°W where the TR joins the GF, which is considered to be seismically inactive (Fig. 1).

The central region (zone III) extends from the GF, which is usually considered to be an extension of the EAF zone, to 11°W longitude (Gorringe Bank; Fig. 1, Table 1). The GF, whose orientation is approximately EW, is clearly marked by bathymetry to 18°W longitude. From this longitude, we observe complex bathymetry dominated by large submarine mountains and abyssal plains, where it is difficult to identify a clear alignment. The GF is a right-lateral transform fault (Buforn et al. 1988) without recent seismic activity (Fig. 1), due to the high return period of larger earthquakes, which may be greater than 80 years and is a period comparable with the existence of instrumental data (Argus et al. 1989). This interpretation is reinforced by the occurrence of several historical earthquakes felt on the Santa Maria Island (Azores) (Nunes et al. 2004; Bezzeghoud et al. 2008). These large earthquakes and the associated seismic deformation may be a result of (1) the long and relative quiescence of the fault or (2) the low seismicity rate or accumulated deformation generated by various

low-magnitude events not detectable by global or regional seismic networks. The GF is characterised by a seismic gap that extends from 23°W to 20°W. From the gap to 11°W, the fault is oriented EW and seismically active, with some large-magnitude events (e.g. M_s 7.1, 20 May 1931; M_w 8.2, 25 November 1941; and M_w 7.9, 25 May 1975).

The seismicity of the Ibero-Maghrebian region (from 11°W to 3.5°E, zones IV, V and VI) is characterised by moderate-magnitude earthquakes, most of which are at shallow depths (≤40 km). The complexity of the region is reflected in its bathymetry, seismicity, stress regime and tectonics, causing it to be divided into three zones, namely zone IV (11°°W–6°W), zone V (6°W–°W) and zone VII (1°W–3.5°E) (Bezzeghoud and Buforn 1999; Buforn et al. 2004). The main feature of the bathymetry is the Gorringe Bank (zone IV), which is located west of the Strait of Gibraltar and contains numerous seamounts, banks and submarine ridges with important regional crustal thickness variations (Torné et al. 2000; Fullea et al. 2007). On land, the main geological features are the Betics, the Rif Cordilleras and the Tell Mountains, which are part of the Alpine domain and formed as a consequence of the collision between the Eu and Nu plates.

West of Gibraltar, from the Gorringe bank to the Gulf of Cadiz region (zone IV), epicentres are distributed in an E-W direction, across an ~100-km-wide band, at shallow and intermediate depths. The region east of 16°W is dominated by a transpressive tectonic regime with a very low convergence rate of 4.3 mm/year, based on a kinematic model (e.g. DeMets et al. 2010; DeMets et al. 1990; Table 1) that trends NW to NNW, consistent with the observed maximum horizontal stress direction (Borges et al. 2001; Bezzeghoud et al. 2008). As noted by DeMets et al. (2010), both models (MORVEL and NUVEL-1A Nubia–Eurasia models) predict rates of motion (4±0.2 mm/year) that differ by only fractions of a millimetre/year everywhere along the plate boundary. For example, along the well-mapped Gloria fault, the velocities given by the two estimates differ by only 0.1 mm/year and 1.0°. However, in region IV, there is no clear plate boundary and the deformation is distributed over a large area reaching a width of 300 km N–S near the continental margin of Iberia. The seismicity is scattered, but most events are concentrated along a 100-km-wide band, trending ESE–WNW from 16°W to 9°W. In this area, WSW–ENE-trending topographic structures have been deformed since the Miocene or earlier (Zittellini et al. 2009). The latter scenario is supported by the occurrence of unusually large oceanic earthquakes within the area of scattered seismicity, such as the M_s 8.0 1969 earthquake (Fukao 1973; Grimison and Cheng 1986; Johnston 1996; López-Arroyo and Udías 1972; Buforn et al. 1988; Grandin et al. 2007a, b), the historical M ~9.0 1755 Lisbon earthquake (e.g. Grandin et al. 2007a, b), and the more recent M 6.0 2007 earthquake (Stich et al. 2007; Pro et al. 2012). Seismic activity at intermediate depths (40 to 150 km depth) is also present in this area (e.g. Buforn et al. 1997). In zone IV, intermediate-depth earthquakes, occurred in 1999, 2002, 2005 and 2011, causing severe damage and deaths in the region (Buforn et al. 2005; Lopez-Comino et al. 2012), are spread over an approximately 100-km-wide band between 36°N and 37°N and extending E–W from 8°W to 11°W.

Zone V is characterised by moderate earthquakes and contains three main concentrations of seismicity at 4°W, where two earthquakes occurred (Al Hoceima, Morocco) on 26 May 1994 (M_w 5.8) and 24 February 2004 (M_w 6.2) (Fig. 1, Table 2). At 2.5°W longitude (south-eastern Spain), a swarm occurred in 1993–1994 with two M 5.0 earthquakes, and at 4.5°W longitude, frequent shocks of m_b ~3 have occurred. In south-eastern Spain, moderate shallow earthquakes (M ≤5.0) occurred in 1999, 2002 and 2005, causing severe damage in the region. This region also has intermediate-depth earthquakes (Buforn et al. 2004) concentrated to the south of Granada, where a large earthquake (M_w 7.8) occurred in 1954 and a M_w 6.2 earthquake occurred in 2010. These are the deepest earthquakes (650 km) in the Mediterranean region, and their origin is still debated (Buforn et al. 2011).

In zone VI, earthquakes are concentrated between 2° and 4° E (El Asnam and Zemmouri-Boumerdes regions, Algeria), where M >6.0 earthquakes occurred on 9 September 1954 (M_s 6.5, El Asnam, formerly Orleanville, Algeria), 10 October 1980 (M_s 7.3, El Asnam, formally Chlef, Algeria), and 21 May 2003 (Zemmouri-Boumerdes, Algeria, M_w 6.8) (Table 2). No intermediate-depth seismic activity is observed in zone VI, east of longitude 3°W in Spain, Morocco and Algeria (Bezzeghoud et al. 1995, 1996; Meghraoui et al. 1986; Buforn et al. 2004; Ayadi et al. 2008).

3 Total seismic moment tensor, seismic slip velocity and slip vector

The total SMT and seismic slip velocities were obtained according the method described in Buforn et al. (2004)

and Borges et al. (2007). Faults and slip vectors along plate boundaries have been used for many years in tectonic interpretation and into many plate-tectonic models (e.g. Minster and Jordan 1978; McCaffrey 1988, 1991; DeMets et al. 1990; DeMets 1993; Udías and Buforn 1991). Two fault parameters are of particular interest: (a) the orientation of fault planes specified by giving the strike and the dip of the plane and (b) the orientation of slip vectors for individual earthquakes. The deduction of stress direction and slip vector from earthquake focal mechanisms is not exempt from ambiguity. As was pointed by several authors (e.g. McKenzie 1969; Udías and Buforn 1991), most earthquakes happen on pre-existing fault planes, and slips can occur at different angles relative to the principal axes. In fact, the maximum compressive stress may have stress an orientation anywhere within the dilatational quadrant, and not necessary at 45° of the fault plane (Udías and Buforn 1991). However, this ambiguity can be resolved using mechanisms of many earthquakes in the same area (e.g. Angelier 1979; Rivera and Cisternas 1990). In our study, there are situations where the focal mechanism was obtained using only the radiation patterns (the oldests). However, in these cases, the plan was chosen closest to the known boundary plates, but for more recent seismic events we have taken into account other analyses such inversion of TMS using extended sources modelling as the distribution of sub-events and directivity study (e.g. Boumerdes earthquake, 2003; Al Hoceima earthquake, 2004; Azores earthquakes, 1997, 1998, 1980). For example, for zones I and II, some of focal mechanisms are obtained from aftershocks study, directivity study or body wave modelling using extended source (1980, 1997, 1998 earthquakes; Hirn et al. 1980; Borges et al. 2007), which allow to decide which is the plane of rupture. In the case of 1980 Azores earthquake, the results of aftershocks study are in agreement with the study of the directivity function of LR waves and distribution of aftershocks (see Borges et al. 2007). In the Gulf of Cadiz–Cape S. Vincent (zone IV), we know the rupture process of several main earthquakes as that of 1969 (e.g. Grandin et al. 2007b) and those of 2003, 2007 and 2009 (e.g. Stich et al. 2007; Pro et al. 2012). For zones V and VI, some solutions are obtained from CMT, body wave modelling using extended source or deduced from InSAR studies (e.g. Bezzeghoud and Buforn 1999; Bounif et al. 2003; Akoglu et al. 2006; Ayadi et al. 2008; Belabbès et al. 2009).

We estimate the slip seismic vector from a selection of $M \geq 5.0$ shallow earthquakes (depth ≤ 40 km) (Fig. 2 and Table 2). The SMTs for the six zones are obtained from all available focal mechanisms (Fig. 2, Table 2) of $M \geq 5.0$ shallow earthquakes and are shown in Fig. 3. For the slip vectors, we assume the same criteria used by Udías and Buforn (1991), where the motion considered for strike-slip faults is in the E–W direction, and for dip-slip faults, the motion corresponds to down-going of the Nu plate with respect to the Eu plate. The direction of seismic slip can be represented as a vector in 3-D space and can be defined by the geometry of the fault plane (the strike φ, the dip δ and the rake λ (direction of slip)) (Aki and Richards 2002), which is measured in the fault plane anticlockwise from the direction of strike. We computed the azimuth of slip vectors in the horizontal plane from the east components of a unit vector in the direction of the earthquake slip vector $(\cos(\varphi)\cos(\delta)\sin(\lambda) + \sin(\varphi)\cos(\lambda))$. In our study, the direction of the slip vectors for the shallow earthquakes is shown corresponding to Africa plate. In order to select the fault plane, we have assumed that the motion in the strike-slip fault is in the E–W direction and in the dip-slip faults, corresponding to down-going of Africa with respect to Eurasia.

3.1 Total seismic moment tensor

In zone I, the SMT corresponds to left-lateral strike-slip faulting with horizontal pressure and tension axes in the E–W and N–S directions, respectively. For zone II, the SMT corresponds to normal faulting, with a horizontal tension axis trending NE–SW, normal to the TR. The rotation of the tension and pressure axes from zone I to zone II is in agreement with the results obtained for morphological features on the linear volcanic ridges. Lourenço et al. (1998) found that the orientation of the spreading axis calculated from the Nuvel-1A model (DeMets et al. 1990) gives a similar value for T axis in both regions, but in our case, the tension axis in zone I is more N–S than in zone II.

Analysis of the SMT of the central region (zone III) shows a strike-slip motion that confirms the homogeneity of the mechanisms of this region, which is already clear from the individual focal mechanisms shown in Fig. 2. In this case, the SMT is controlled by the $M \geq 7.0$ events (Table 2) in this region.

For zone IV, the SMT corresponds to thrusting with the horizontal pressure axis oriented NNW–SSE because of to the solution of the 1969 earthquake. A

similar result was obtained for zone VI; the SMT shows thrusting from the M >6.0 earthquakes in the El Asnam region in 1954 and 1980.

Because of the complexity of zone V, we present only the part that corresponds to the Alboran Sea and Morocco, where the SMT shows strike-slip motion with a horizontal tension axis oriented NE–SW. However, from Fig. 2, as was pointed by Buforn et al. (2004), we observe that area V differs from IV and VI, where the predominant motion is of reverse character with an average horizontal compression in the NNW–SSE direction. In area V, focal mechanisms show a greater variety of solutions, which corresponds to normal faulting, strike-slip mechanisms with a large component of normal motion, reverse faulting, strike-slip with a large component of reverse motion and pure strike-slip faulting. There exist some strike-slip mechanisms in IV and in V, which are also compatible with a horizontal compression in the NNW–SSE direction. Strike-slip solutions have a predominantly E–W plane with right-lateral motion, the northern block moving east. Thus, a normal component of motion is present in several shocks. Most solutions in area IV are compatible with a stress pattern consisting of a general horizontal tension axis in the E–W direction and a horizontal pressure axis in the NW–SE direction. Solutions with a large normal component and vertical P axis are more frequent on the south coast of Spain and in the Alboran Sea (Buforn et al. 2004).

Thus, in the three zones (IV, V and VI), there is a common orientation of the pressure axis, which is horizontal and trending N–S to NW–SE. The tension axis is nearly vertical in zones IV and VI, nearly horizontal in V and trending E–W to NE–SW.

The values of the non-double couple (CLVD) components are small for the six zones and are between 0.3 % (zone III) and 12 % (zone II). These small values confirm that these solutions are very similar and that large earthquakes control the stress regime (Buforn et al. 2004; Bezzeghoud et al. 2008).

3.2 Seismic slip velocity

The average slip velocities for these six zones were first estimated by Buforn et al. (2004, zones IV, V and VI), Bezzeghoud et al. (2008) and Buforn (2008).

These values were determined from the moment rate using data from $M_s \geq 4.0$ earthquakes (see references in Table 2). The moment rate, M_o, was estimated from the sum of the scalar seismic moment in each area divided by the time period according the method described in Buforn et al. (2004) and Borges et al. (2007). For earthquakes without an estimate of seismic moment in the Azores region (zones I and II), an empirical relationship between M_o and M_s has been derived ($\log M_o = 1.1 M_s + 11$; Borges et al. 2007), based on $M_s \geq 4.4$ earthquakes in the instrumental period (1973–1997) (Borges 2003). This estimate covers a period of 87 years (1923–2010), and the seismogenic area corresponds to a vertical fault 10 km in width and 172 and 250 km in length for zones I and II, respectively. For zones IV, V and VI, the moment rate was estimated using $m_b \geq 5.0$ shallow earthquakes in each area from 1900 to 2010. We used an empirical relationship between the magnitude, m_b, and scalar seismic moment ($\log M_o = 1.54 m_b + 8.7$; Buforn et al. 2004), M_o, obtained from events with values determined from the spectra of body waves obtained by Buforn et al. (2004). We took the area of a vertical fault with the same length for zones IV and V (550 km) and a length of 440 km for zone VI, with a width of 10 km (the average depth of shallow earthquakes). This is equivalent to considering a fault with these dimensions as the origin of the shallow seismicity ($M \geq 4.4$, see references in Table 2).

Based on these hypotheses, we obtained the following seismic slip velocities. In zone I, a slip velocity of 6.7 mm/year versus 3.1 mm/year in zone II shows higher seismic activity in zone I (Table 2).

Because of the small number of events in the central region, the slip velocity was estimated using the M_s/M_o relationship, given by Buforn et al. (1988), for the whole Azores-Gibraltar region. For the central region (zone III), we obtain a slip velocity of 18 mm/year, which is in agreement with the large earthquakes that occurred in this zone.

For areas IV, V and VI, the calculated slip velocities are 5.5, 1.4 and 3.7 mm/year, respectively. The values for zones IV and VI are conditioned by the large earthquakes in each region (1964 and 1969 Gulf of Cadiz earthquakes in zone IV, and 1954 and 1980 El Asnam region earthquakes, and 2003 Boumerdes earthquake in zone VI). However, the slip velocity for zone V is nearly 5 orders of magnitude lower than that for zone IV and about 2.5 orders of magnitude lower than that for zone VI because of the lack of larger earthquakes during the last 120 years in zone V, where the maximum magnitudes are about 6 (M 6.2, 2004 Alhoceima earthquake). The average slip velocities are shown in Fig. 3 and listed in Table 1.

Changes in the focal mechanisms along the Azores–Gibraltar–Algeria Plate boundary region show that the

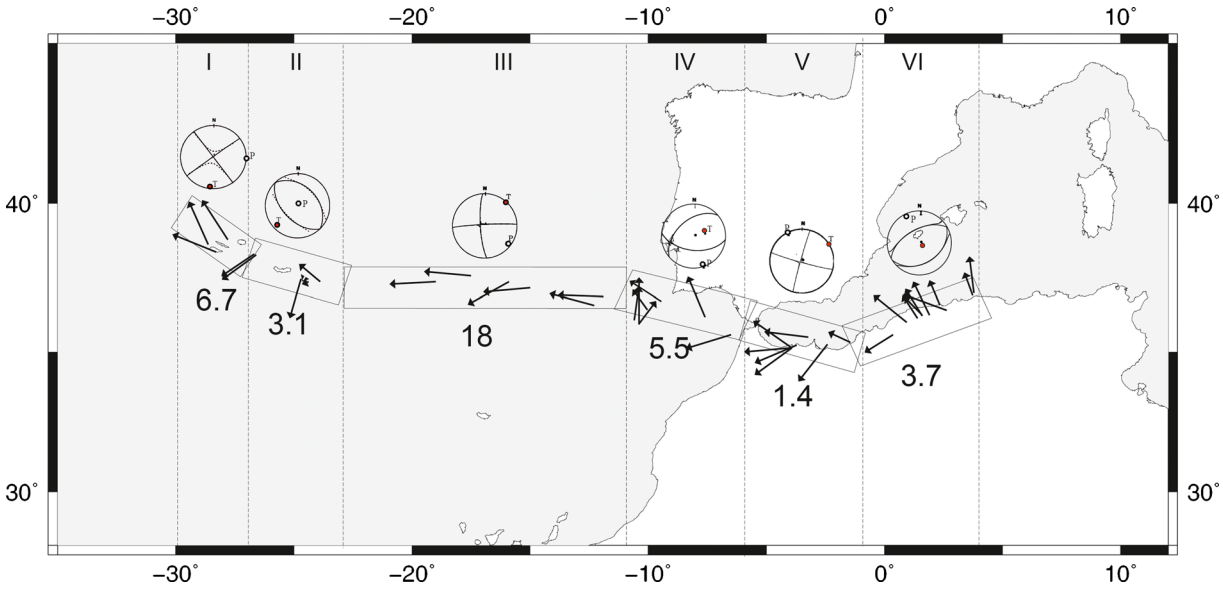

Fig. 3 The total seismic moment tensor and horizontal projection of the slip vectors for shallow earthquakes (depth ≤40 km; $M \geq 5.5$) in the six studied zones corresponding to the Nubia plate boundary. Slip velocities obtained from the seismic strain of shallow earthquakes are indicated along the boundary. Slip velocity was estimated from the moment rate according to the expression $\Delta\dot{u} = \dot{M}_o/\mu A$, where μ is the rigidity coefficient and A the fault area represented by the rectangle in each zone. See the text for more details. The Roman numerals (*I* to *VI*) indicate the six zones studied and described in the text

present plate motion is transtensional in the Azores, dextral along the Gloria transform and convergent between the SW Atlantic margin and the Ibero-Maghrebian region (Figs. 1, 2 and 3). An important point is that the energy released by aseismic folding, thickening, plastic deformation or slow aseismic slippage is not included in our estimation of slip velocity, which means that seismic strain analyses underestimate the geological deformation. The velocity used in this work may be considered to be instantaneous and independent from that derived from geodetic data. In addition, the slip rate assumes that the earthquake cycle is much shorter than the history of available earthquakes (Borges et al. 2007). The adequacy of seismic catalogues to estimate earthquake recurrence rate depends on the area of the region, catalogue duration and regional strain rates (Ward 1998). Given the short catalogue duration and variability in absolute rates, spatial similarity between geodetic deformation and seismicity is not necessarily expected (Borges et al. 2007, 2008).

3.3 Slip vector

The directions of the slip vectors relative to the Eurasia plate for shallow earthquakes (depth ≤40 km) with a significant magnitude ($M \geq 5.5$) (Table 2) are shown in Figs. 3 and 4. From North Algeria to the MAR, the predominant slip vectors display several directions. In North Algeria, the observed NW slip indicates compression in this direction. In north Morocco and the Alboran Sea, the slip vectors are oriented W–SW, and they rotate to N–NW in the Gulf of Cádiz. Along the Gloria Fault, the slip vector is oriented E–W. In the Azores, there are two different vector sets: a SW-oriented vector at the TR and an NW-oriented vector near the MAR. For slip vectors derived from focal mechanisms, zones II, IV and VI show homogenous slip directions. Zones I, II and V present more variety in the slip vectors, which shows the complexity of these zones.

4 Kinematic models

The kinematic models provide the motion of a lithospheric plate in a given reference frame. In this study, we consider the relative motion between the Eu and Nu plates. A wide variety of kinematic models is available, but we can classify them into two types: geological models and geodetic models. The geological models use mainly magnetic profiles to derive seafloor-spreading rates and azimuths of transform faults. These models provide a plate velocity averaged over a

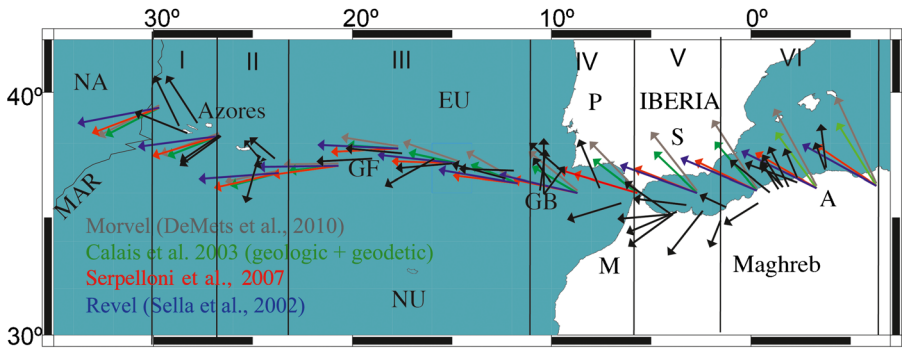

Fig. 4 Slip vectors deduced from seismicity (in *black*, see text) and relative kinematic velocities between the Eu and Nu plates, calculated from several models

few million years. For example, Nuvel-1A (DeMets et al. 1994), which is one of the most famous geological models, is derived from the magnetic anomaly 2A (representing the 3 Myr isochron) and thus describes the relative Eurasia–Nubia (Eu–Nu) velocity averaged over 3 Myr. Geodetic models have the potential to measure relative plate motions over periods of just a few years and are mainly based on GPS data.

In Fig. 4, we display the Morvel model (DeMets et al. 2010) in grey, which is the latest update of the Nuvel-1A geological model (DeMets et al. 1994). The REVEL-2000 geodetic model (Sella et al. 2002) is also displayed in blue. REVEL-2000 is a new model for recent plate motion of 19 plates and is based on space-geodetic data, primarily GPS ones, from 1993 to 2000. The kinematic model of Serpelloni et al. (2007) (in red, Fig. 4) integrates continuous GPS observations with data acquired during repeated campaigns of temporary geodetic stations in regional, subregional and local networks around the Eurasia–Nubia plate boundary. Calais et al. (2003) concentrate on the relative motion of the Nubia, Eurasia and North America plates, and provide a geological model, a geodetic model and a model combining geological and geodetic data. The latter is displayed in green in Fig. 4.

These models show similar patterns of the relative velocity between the Eu and Nu plates (Fig. 4). In the easternmost part of the study area, i.e. in western Algeria, the kinematic relative velocity has a NNW orientation. These vectors become more oblique until reaching the GF. Along the GF, we observe an anticlockwise rotation between NNW and NW. West of this location, the vectors have a constant orientation. The pattern is well recovered in all of the considered models. However, the obliqueness of the vectors varies among models. Specifically, the geodetic models provide relative velocities that are generally more oblique than those obtained from the geological models, which produces a real change in the relative Eu–Nu motion. According to Calais et al. (2003), the direction of the Eu–Nu convergence has rotated 20° anticlockwise in the past few million years.

5 Correlation of slip kinematic velocities

We investigate here how the relative kinematic velocities between the Eurasia–Nubia plates correlate with the seismic slip vectors. This comparison is qualitative because the slip norms are only indicative of the fault angle, but it can provide important information on the ongoing crustal deformation. In Fig. 4, we superpose relative velocities with slip vectors. At a global scale (Eu and Nu plates), we obtain a good correlation between these vectors. In western Algeria, the two vector sets have the same direction. In the Alboran Sea, there is a complete lack of correlation, which will be discussed later. However, the anticlockwise rotation along the GF is well reproduced. Along the TR, the direction is partially correlated.

The complete lack of correlation in direction in the Alboran Sea may be explained by the complexity of this region, as several phenomena seem to overlap there. Jimenez-Munt et al. (2001) study the stress partitioning through the thin-sheet approach and propose that the stress pattern of the Alboran Sea is best explained if this region is considered to be an independent microplate. The geodetic study of Vernant et al. (2010) invokes mantle dynamics and slab rollback to account for the observed motions. The geodynamic model of Pérouse et al. (2010) demonstrates that simple Eu–Nu convergence is not sufficient to account for the complex

surface deformation and that a sub-crustal or sub-lithospheric forcing, representative of the delamination and rollback of the subducted African lithosphere, is required. This finding explains the difference between the slip vector and the kinematic vectors, which are only representative of the Eu–Nu convergence. Note that the output of the Pérouse et al. (2010) model is very similar to the slip velocities inferred in this study, thus demonstrating their physical pertinence.

In the Gulf of Cadiz, the earthquakes from which the slip mechanisms were derived display thrust faulting. The slip directions are N, NNW, NE and WWS. None of these directions correspond to the directions inferred from the relative kinematic velocities. These directions are actually quite similar to the dextral SW Iberian margin faults described by Zittellini et al. (2009) from a multibeam bathymetry compilation. This correlation is puzzling because the present deformation occurs only along reverse faults.

In the Azores and along the TR, the direction of the slip vectors is partially recovered by the kinematic velocities. For example, in zone I, the directions of the slip are quite close to the relative velocity provided by Calais et al. (2003). In the northern Azores Islands (Sao Jorge, Faial, Terceira), the relative kinematic velocities show a SW–SWW direction, whereas the directions of the slip are N300 and N330. However, the latter directions are supported by a study based on the regional morphology (Lourenço et al. 1998). Lourenco et al. (1998) show that the Azores triple junction is controlled by two sets of conjugate faults oriented N150 and N120. The slip vectors presented in this study (Fig. 3) correspond to motion along these faults. Difference from the relative Eu–Nu relative kinematic velocities can be explained by accommodation of competing forces among the three plates (Eu, Nu and NA), instead of only two. Let us note that the strong correlations between observed tectonic stress and absolute plate motions shown by the World Stress Map Project point directly to the present lithospheric stress fields being dominated by the individual plate boundary and body forces (Zoback et al. 1989; Zoback 1992). However, most researchers believe that the mantle forces related to large convection cells must dominate the driving forces (Jacoby 1980; Carlson et al. 1983; Wilson 1993; Ziegler 1993). So, in a sense, through time the dominant forces will change from plate to mantle and back.

However, except for these local departures explained by the superposition of different phenomena, the directions of the slip vectors and, more importantly, the changes in the slip direction are well reproduced by the relative kinematic velocities of the Eu and Nu plates.

6 Quantitative study

For a more quantitative study, we compare the kinematic velocities with the slip velocities deduced from the seismicity (Figs. 3 and 4, Table 1). In Fig. 5, we report the velocities as a function of longitude in the study area. The norms of the relative kinematic velocities are in the same range as the slip velocities. They range between 2 and 7 mm/year, with the exception of an outlier in zone III that displays a much higher value (18 mm/year). Other than similar norms, we do not find a correlation between the slip velocities and the kinematic velocities.

If the relative kinematic velocities between the Eurasia–Nubia plates are converted to a force applied to this physical boundary, it makes sense to consider the physical characteristics of this boundary. These characteristics vary greatly in the study area, as illustrated in the lower panel of Fig. 5, where the crustal thickness (Jimenez-Munt et al. 2001) is interpolated along the geological track that is the potential limit between the Eu and Nu plates (Bird 2003). Note that the study of Jimenez-Munt et al. (2001) does not encompass the entire study area. Therefore, east of 0° longitude, we assume a constant crustal thickness, and west of 25°W longitude, we extrapolate the crustal thickness by performing a linear interpolation between thicknesses of 15 km (the value they provide at longitude 25°W) and 6 km (the value generally found near a mid-ocean ridge). The crustal thickness along this boundary displays significant variations, ranging from 6 to 35 km. The slip velocities seem to be larger for a thicker crust.

The variation in bathymetry along this boundary (Fig. 5c) displays some correlation with the regional tectonic regimes. The decrease of the bathymetry between zones I and II arises from the thermal cooling of the lithosphere and cannot be directly interpreted in terms of change in the regional stress regime. The increase in slip velocity between zones II and III is correlated with an increase of the bathymetry. If this bathymetric feature is not of volcanic origin, this correlation can be explained by a change in the tectonic regime. Zone II is associated with normal and strike-slip motion (for which we expect a bathymetric low), whereas in

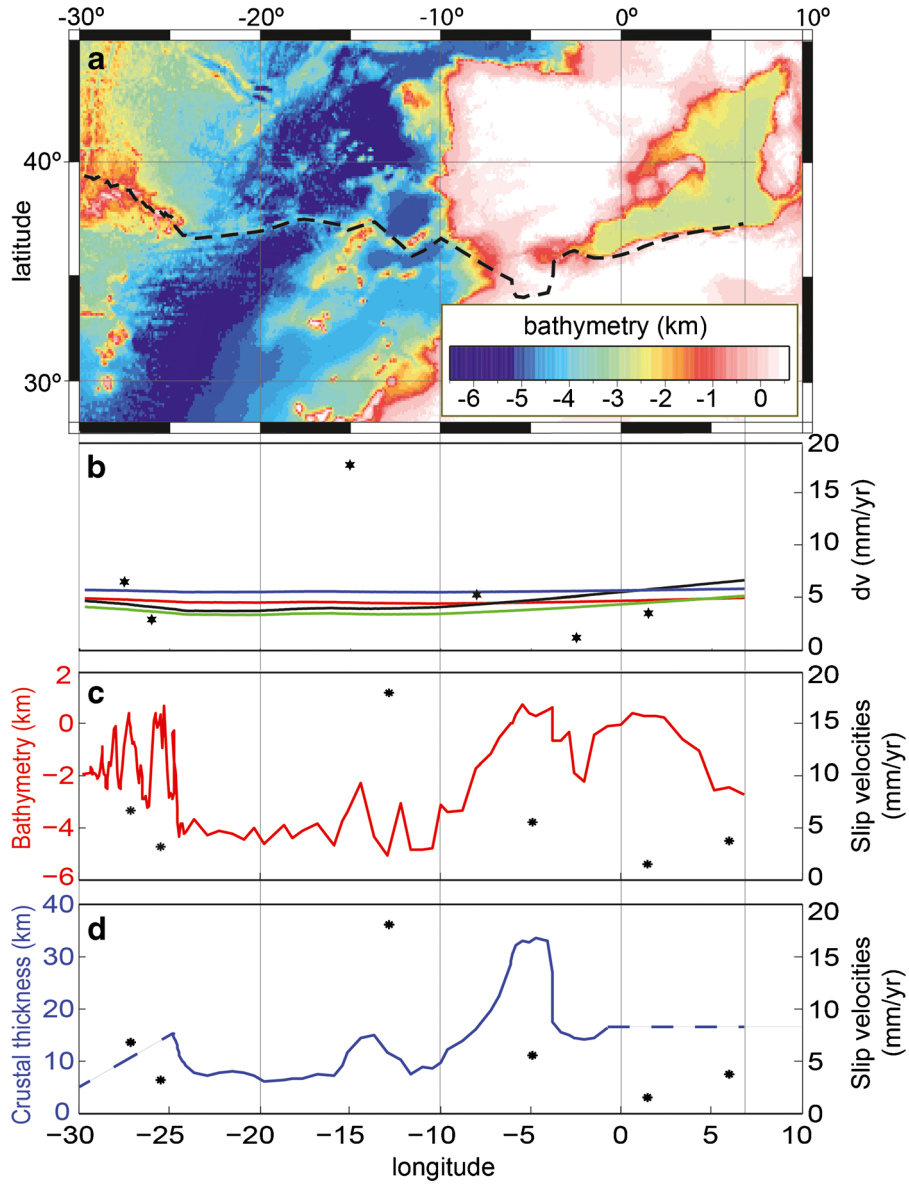

Fig. 5 **a** *Top*, bathymetry of the study area (Smith and Sandwell 1997). **b** Norm of the slip velocities (*black* stars) and the relative kinematic velocities (*coloured lines*) as a function of longitude in the study area. Morvel (DeMets et al. 2010) is represented in *grey*, the model from Serpelloni et al. (2007) is in *red*, the mixed geological and geodetic model from Calais et al. (2003) is in *green*, and the Revel model (Sella et al. 2002) is in *blue*. **c** The *solid red* line shows the bathymetry along the geological track (Smith and Sandwell 1997). **d** The *solid line* represents the crustal thickness along the same track (Jimenez-Munt et al. (2001)). The *stars* represent the mean slip velocity deduced from the seismic moments for each of the six areas identified in this study (see text, Fig. 3 and Table 1)

zone III, there is a combination of strike-slip and reverse fault motions, which would induce an increase in bathymetry (e.g. Lammali et al. 1997).

In zone V, the plate boundary is more diffuse and corresponds to a wide area encompassing the Betics-Rif orogenic arc and the Alboran Sea. The stresses are released by frequent small-to-moderate earthquakes involving normal and strike-slip faults. According to the previous discussion, this region would be expected to be associated with a bathymetric low, but a bathymetric high is actually observed. The bathymetry in zone V seems to be controlled by a more complex tectonic

regime than that in zones IV and VI, as shown by the singularity of the SMT and the slip vectors in Fig. 3.

Bezzeghoud and Buforn (1999) suggest that this contrast could be related to the difference between the continental domain to the west (Alboran domain) and the oceanic domain in the east (Algerian basin). The large seafloor relief and the high seismicity observed in the Alboran Sea with respect to the absence of both in the Algerian basin emphasise the difference in crustal structure to either side of zone V.

As previously mentioned, when the relative kinematic velocities between the Eu and Nu plates are assimilated to a force applied on this physical boundary, it is important to account for the morphology of this margin and determine how the displacement should be adjusted based on this morphology. It seems physically reasonable that the seismic displacement should be greater if the crust is thin because it faces less resistance to the applied forces. Let us note that the maximum depth of earthquake in the crust, which defines the thickness of the seismogenic layer in the studied area, is of the order of 10 to 30 km. This gives us a scale for quantification of the dimensions of seismic structures in the region. Earthquakes capable to break the entire thickness of the seismogenic zone can be considered as larges events, and those with ruptures confined within the seismogenic zone can be considered as moderate-size events. It then is more logical to consider the norm of the relative kinematic velocities, normalised by the crustal thickness (i.e. divided by the thickness of the crust) and multiplied by the mean crustal thickness over the considered profile. The reference crustal thickness (15 km) is the mean crustal thickness along the Eu–Nu boundary. For each of the six zones, we compute the mean relative kinematic velocity normalised by the crustal thickness. These values are displayed in Fig. 6 as a function of the mean slip velocities deduced from the seismic moment tensor (Table 1 and Fig. 3). A linear trend arises from this comparison. However, the two mean velocity sets are not exactly equal, as their relationship has a slope of 0.2 and a *y*-intercept of 3.4–4 mm/year. The reason why the slope is not unity may be that only 20–30 % of the energy released by an earthquake is released through mechanical waves (Kanamori 2001). The *y*-intercept may indicate that a threshold value of the applied force is required before any motion occurs. For forces lower than this threshold, the motion may be aseismic, as discussed by Bird et al. (2009).

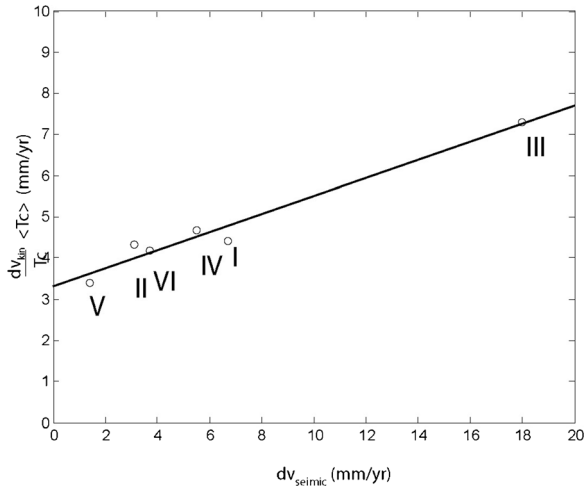

Fig. 6 Relative kinematic velocity normalised by the crustal thickness versus slip velocity deduced from seismic moments. Each of the six values is representative of the mean value found for the six zones of coherent seismicity identified in this study and is denoted by *Roman numerals*

7 Conclusions

Our study concerns the complex seismicity pattern along the western part of the Eurasia–Nubia plate boundary. To better characterise the seismicity, we propose a new seismotectonic synthesis based on the analysis of shallow $M \geq 5.0$ earthquakes (depth ≤ 40 km), occurring between 1931 and the present time. We show that the study area can be divided into six zones of coherent seismicity, for which we provide the SMT and the average slip velocities.

As the factors controlling the seismicity pattern are not yet well understood, we determined the extent to which the patterns are controlled by the kinematics of global plates. We investigate the correlation between the slip vectors, which are computed from the focal mechanisms of several events, with the relative kinematic velocities derived from global kinematic models. We show that despite some local departures, the direction of the slip vector and, more importantly, the change in the slip direction are well reproduced by the relative kinematic velocity between the Eu and Nu plates. The departures in the Alboran Sea and at the Azores Triple Junction have been explained by the interaction of other phenomena. Quantitatively, the slip velocities display a linear, non-affine correlation with the norms of the relative kinematic velocities, modulated by the lithosphere structure. The norm of the slip velocities seems

to depend on the tectonic regime and on the morphology of the plate boundary.

Acknowledgments This work has been developed with the support of 1) the Fundação para a Ciência e Tecnologia (FCT/MCTES, Portugal) through the projects PTDC/GEO-FIQ/3522/2012, PTDC/CTE-GIX/101852/2008, PEst-OE/CTE/UI0078/2011; 2) the "Agence Universitaire de la Francophonie (AUF)" through the project "Coopération scientifique interuniversitaire (PCSI)"; 3) the Ministerio de Ciencia e Innovación (Spain) through the project CGL2010-19803- C03-01. CA is "Ciência FCT researcher" funded by the European Social Fund and MCTES Portugal Funds. This article benefited a lot from suggestions provided by two anonymous reviewers.

References

Aki K, Richards PG (2002) Quantitative seismology, theory and methods. 2nd edn. University Science Books, Sausalito, CA, 700 p

Akoglu AM, Cakir Z, Meghraoui M, Belabbes S, El Alami SO, Ergintav S, Akyüz S (2006) The 1994–2004 Al Hoceima (Morocco) earthquake sequence: conjugate fault ruptures deduced from InSAR. Earth Planet Sci Lett 252:467–480

Altamimi Z, Sillard P, Boucher C (2002) ITRF2000: a new release of the international terrestrial reference frame for earth science applications. J Geophys Res 107(B10):2214. doi:10.1029/2001JB000561

Angelier J (1979) Determination of the mean principal directions of stresses for a given fault population. Tectonophysics 56: T17–T26

Argus D, Gordon R, DeMets C, Stein S (1989) Closure of the Africa–Eurasia–North America plate motion circuit and tectonics of the Gloria fault. J Geophys Res 94:5585–5602

Ayadi et al (2003) Strong Algerian earthquake strikes near capital city. Eos Trans AGU 84(50):561–568

Ayadi A, Dorbath C, Ousadou F, Maouche S, Chikh M, Bounif MA, Meghraoui M (2008) Zemmouri earthquake rupture zone (Mw 6.8, Algeria): aftershocks sequence relocation and 3-D velocity model. J Geophys Res 113, B09301

Belabbès S, Wicks C, Çakir Z, Meghraoui M (2009) Rupture parameters of the 2003 Zemmouri (M_w 6.8), Algeria, earthquake from joint inversion of interferometric synthetic aperture radar, coastal uplift, and GPS. J Geophys Res 114: B03406. doi:10.1029/2008JB005912

Benouar D (1994) Materials for the investigation of the seismicity of Algeria and adjacent regions during the twentieth century, special issue of the Annali Di Geofisica, Vol. XXXXVII, No 4

Bezzeghoud M, Buforn E (1999) Source parameters of 1992 Melilla (Spain, Mw=4.8), 1994 Alhoceima (Morocco, Mw=5.8) and 1994 Mascara (Algeria, Mw=5.7) earthquakes and seismotectonic implications. Bul Seis Soc Am 89(2): 359–372

Bezzeghoud M, Dimitrov D, Ruegg JC, Lammali K (1995) Faulting mechanism of the El Asnam (Algeria) 1954 and 1980 earthquakes from modelling of vertical movements. Tectonophysics 249:249–266

Bezzeghoud M, Ayadi A, Sébaï A, Aït Messaoud M, Mokrane A, Benhallou H (1996) Seismicity of Algeria between 1365 and 1989: map of maximum observed intensities (MOI). Avances en Geofísica y Geodesia Pub de IGN (Madrid) I:107–114

Bezzeghoud M, Borges JF, Caldeira B, Buforn E, Udias A (2008) Seismic activity in the Azores Region in the context of the western part of the Eurasia–Nubia plate boundary. International Seminar on Seismic risk and rehabilitation on the 10th Anniversary of the July 9 1998 Azores Earthquake, Horta-Azores, 9–13 July. p. 27–31

Bird P (2003) An updated digital model of plate boundaries. Geochem Geophys Geosyst 4(3):1027. doi:10.1029/2001GC000252

Bird P, Kagan YY, Jackson DD, Schoenberg FP, Werner MJ (2009) Linear and nonlinear relations between relative plate velocity and seismicity. Bulletin of the Seis 99(6):3097–3113. doi:10.1785/0120090082

Borges J (2003) Fonte sísmica em Portugal. Algunas implicaçoes na Geodinâmica Açores-Gibraltar. Ph.D., University of Evora, Portugal, 307 pp

Borges JF, Fitas AJS, Bezzeghoud M, Teves-Costa P (2001) Seismotectonics of Portugal and its adjacent Atlantic area. Tectonophysics 337:373–387

Borges JF, Bezzeghoud M, Buforn E, Pro C, Fitas AJS (2007) The 1980, 1997 and 1998 Azores earthquakes and its seismotectonic implications. Tectonophysics 435:37–54

Borges JF, Caldeira B, Bezzeghoud M. e E. Buforn (2008) Seismicity and seismotectonics of Azores: geodynamic implications, Ch. 6, 99-110, in a Oliveira C. S., Costa A. and J. C. Nunes (Eds.), A book on the 1998 Azores earthquake—10 years after it's occurrence, ISBN 978.989-20-1223-0, 741p

Bounif A, Bezzeghoud M, Dorbath L, Legrand D, Deschamps A, Rivera L, Benhallou H (2003) Seismic source study of the 1989, October 29, Chenoua (Algeria) earthquake from aftershocks, broad- band and strong ground motion records. Ann Geophys 46(4):625–646

Buforn E (2008) Seismotectonics of Azores-Tunisia. In: L. Mendes-Victor, C. Sousa Oliveira, J. Azevedo, A. Ribeiro (Eds). The 1755 Lisbon Earthquake Revisited 397-410

Buforn E, Udías A, Colombás MA (1988) Seismicity, source mechanisms and seismotectonics of the Azores-Gibraltar plate boundary. Tectonophysics 152:89–118

Buforn E, Sanz DE, Galdeano C, Udias A (1995) Seismotectonics of the Ibero-Maghrebian Region. Tectonophysics 248:247–261

Buforn E, Coca P, Udías A, Lasa C (1997) Source mechanism of intermediate and deep earthquakes in southern Spain. J Seism 1:113–130

Buforn E, Bezzeghoud M, Udías A, Pro C (2004) Seismic sources on the Iberia-African plate boundary and their tectonic implications. Pure Appl Geophys 161:623–646

Buforn E, Benito B, Sanz De Galdeano C, del Fresno C, Muñoz D, Rodriguez I (2005) Study of the damaging earthquakes of 1911, 1999, and 2002 in the Murcia, Southeastern Spain, Region: seismotectonic and seismic-risk implications. Bull Seism Soc Am 95:549–567. doi:10.1785/0120040041

Buforn E, Pro C, Cesca S, Udías A, del Fresno C (2011) The 2010 Granada (Spain) deep earthquake. Bull Seism Soc Am 101: 2418–2430. doi:10.1785/0120110022

Calais E, DeMets C, Nocquet J-M (2003) Evidence for a post-3.16-Ma change in Nubia–Eurasia–North America plate motions? Earth Panet Sci Lett 216:81–92

Carlson RL et al (1983) The driving mechanism of plate tectonics: relation to age of the lithosphere at trenches. Geophys Res Lett 10:297–300

DeMets C (1993) Earthquake slip vectors and estimates of present-day plate motions. J Geophys Res 98(B4):6703–6714

DeMets C, Gordon R, Argus A, Stein A (1990) Current plate motions. Geophys J Int 101:425–478

DeMets C, Gordon RG, Argus DF, Stein S (1994) Effect of recent revisions to the geomagnetic reversal time scale on estimates of current plate motions. Geophys Res Lett 21:2191–2194

DeMets C, Gordon RG, Argus DF (2010) Geologically current plate motions. Geophys J Int 181(1):1–80. doi:10.1111/j.1365-246X.2009.04491.x

Fernandes RMS, Ambrosius BAC, Noomen R, Bastos L, Wortel MJR, Spakman W, Govers R (2003) The relative motion between Africa and Eurasia as derived from ITRF2000 and GPS data. Geophys Res Lett 30(16):1828. doi:10.1029/2003GL017089

Fukao Y (1973) Thrust faulting at a lithospheric plate boundary the Portugal earthquake of 1969, Earth Planet. Sci Lett 18: 205–216. doi:10.1016/0012-821X(73)90058-7

Fullea J, Fernandez M, Zeyen H, Vergés J (2007) A rapid method to map the crustal and lithospheric thickness using elevation, geoid anomaly and thermal analysis. Appl Gibraltar Arc Syst Atlas Mountains Adjacent Zones Tectonophysics 430:97–117

Grandin R, Borges JF, Bezzeghoud M, Caldeira B, Carrilho F (2007a) Simulations of strong ground motion in SW Iberia for the 1969 February 28 (M_S=8.0) and the 1755 November 1 (M~8.5) earthquakes– I. Velocity model

Grandin R, Borges JF, Bezzeghoud M, Caldeira B, Carrilho F (2007b) Simulations of strong ground motion in SW Iberia for the 1969 February 28 (M_S=8.0) and the 1755 November 1 (M~8.5) earthquakes—II. Strong ground motion simulations. Geophys J Int 171(2):807–822

Grimison N, Cheng W (1986) The Azores-Gibraltar plate boundary: focal mechanisms, depths of earthquakes and their tectonic implications. J Geophys Res 91:2029–2047

Hirn A, Haessler J, Hoang Trong P, Wittlinger G, Mendes Victor L (1980) Aftershock sequence of the January 1st, 1980 earthquake and present-day tectonics in the Azores. Geophys Res Lett 7:501–504

Jacoby WR (1980) Plate sliding and sinking in mantle convection and the driving mechanism, In: Davis, P.A., Runcorn, F.R.S. (eds) Mechanisms of Continental Drift and Plate Tectonics, Academic Press, New York, p 159–172

Jimenez-Munt I, Fernandez M, Torneand M, Bird P (2001) The transition from linear to diffuse plate boundary in the Azores-Gibraltar region: results from a thin-shit model. Earth Panet Sci Lett 192:175–189

Johnston A (1996) Seismic moment assessment of earthquakes in stable continental regions—III. New Madrid 1811–1812, Charleston 1886 and Lisbon 1755. Geophys J Int 126:314–344

Kanamori H (2001) Energy budget of earthquakes and seismic efficiency. In: Teisseyre R, Majewski E (eds) Earthquake thermodynamics and phase transformations in the earth's interior. Academic Press, New York, pp 293–305

Lammali K, Bezzeghoud M, Oussadou F, Dimitrov D, Benhallou H (1997) Postseismic deformation at El Asnam (Algeria) in the seismotectonics context of North Western Algeria. Geophys J Int 129:597–612

López-Arroyo A, Udías A (1972) Aftershock sequence and focal parameters of the February 28th, 1969 earthquake of the Azores-Gibraltar Fracture Zone. Bull Seism Soc Am 62(3): 699–720

Lopez-Comino J, Mancilla F, Morales J and Stich D (2012) Rupture directivity of the 2011, Mw=5.2 Lorca earthquake (Spain). Geophys Res Lett 39 doi:10.1029/2011GL050498

Lourenço N, Miranda JM, Luis JF, Ribeiro A, Mendes Victor LA, Madeira J, Needham HD (1998) Morpho-tectonic analysis of the Azores Volcanic Plateau from a new bathymetric compilation of the area. Mar Geophys Res 20:141–156

Machado F (1966) Contribução para o estudo do terremoto do terramoto de 1 de Novembro de 1755. Rev Fac Ciências Lisbon C 14:19–31

Madeira J, Ribeiro A (1980) Geodynamics models for the Azores triple junction: a contribution from tectonics. In: G. Boillot and J.M. Fontboté (eds), Alpine evolution of Iberia and its continental margins. Tectonophysics 184, 405-415

Martínez-Solares JM, Lopez-Arroyo A (2004) The great historical 1755 earthquake. Effects and damage in Spain. J Seismol 8(2):275–294

McCaffrey R (1988) Active tectonics of the eastern Sunda and Banda arcs. J Geophysical Res 93:15163–15182

McCaffrey R (1991) Slip vectors and stretching of the Sumatran fore arc. Geology 19:881–884

McKenzie DP (1969) The relationship between fault plane solutions for earthquakes and the directions of the principal stresses. Bull Seismol Soc Am 59:591–601

McKenzie D (1972) Active tectonics of the Mediterranean region. Geophys J R Astron Soc 30:109–185

Meghraoui M, Pondrelli S (2012) Active faulting and transpression tectonics along the plate boundary in North Africa. Ann Geophys 55:5. doi:10.4401/ag-4970

Meghraoui M, Cisternas A, Philip H (1986) Seismotectonics of the lower Chelif basin: structural background of the El-Asnam (Algeria) earthquake. Tectonics 5:809–836

Minster JB, Jordan TH (1978) Present-day plate motion. J Geophys Res 83:5331–5354

Moreira VS (1985) Seismotectonics of Portugal and its adjacent area in the Atlantic. Tectonophysics 117:85–96

Nunes JC, Forjaz VH, Oliveira CS (2004) Catálogo Sísmico da Região dos Açores. Versão 1.0 (1850-1998). Universidade dos Açores (Ed.). Ponta Delgada. Edição CD-ROM. ISBN: 972-8612-17-6

Pérouse E, Vernant P, Chéry J, Reilinger R, McClusky S (2010) Active surface deformation and sub-lithospheric processes in the western Mediterranean constrainted by numerical models. Geology, 38 (9), doi:10.1130/G30963.1

Pro C, Buforn E, Bezzeghoud M, Udias A (2012) The earthquakes of 29 July 2003, 12 February 2007, and 17 December 2009 in the region of Cape Saint Vincent (SW Iberia) and their relation with the 1755 Lisbon earthquake. Tectonophysics 583:16–27. doi:10.1016/j.tecto.2012.10.010

Rivera L, Cisternas A (1990) Stress tensor and fault-plane solutions for a population of earthquakes. Bull Seismol Soc Am 80:600–614

Searle R (1980) Tectonic pattern of the Azores spreading centre and triple junction. Earth Plan Sci Lett 51:415–434

Sella GF, Dixon TH, Mao A (2002) REVEL: a model for recent plate velocities from space geodesy. J Geophys Res 107(B4): 2081. doi:10.1029/2000JB000033

Serpelloni E, Vannucci G, Pondrelli S, Argnani A, Casula G, Anzidei M, Baldi P, Gasperini P (2007) Kinematics of the Western Africa–Eurasia plate boundary from focal mechanisms and GPS data. Geophys J Int 169:1180–1200. doi:10.1111/j.1365-246X.2007.03367

Smith WHF, Sandwell DT (1997) Global seafloor topography from satellite altimetry and ship depth soundings. Science 277:1957–1962

Stich D, Mancilla F, Pondrelli S, Morales J (2007) Source analysis of the February 12th 2007, Mw 6.0 horseshoe earthquake: implications for the 1755 Lisbon earthquake. Geophys Res Lett 34. doi:10.1029/2007GL0300127

Torné M, Fernàndez M, Comas MC, Soto JI (2000) Lithospheric structure beneath the Alboran Basin: results from 3D gravity modeling and tectonic relevance. J Geophys Res 105:3209–3228

Udías A (1980) Seismic stresses in the region Azores–Spain–Western Mediterranean. Rock Mech 9:75–84

Udías A, Buforn E (1991) Regional stresses on the Eurasia Africa plate boundary derived from focal mechanisms of large earthquakes. Pageoph N 136:433–448

Udías A, Lopez Arroyo A, Mezcua J (1976) Seismotectonic of the Azores-Alboran region. Tectonophysics 31:259–289

Vernant P, Fadil A, Mourabit T, Ouazar D, Koulali A, Davila JM, Garate J, McClusky S, Reilinger R (2010) Geodetic constraints on active tectonics of the Western Mediterranean: implications for the kinematics and dynamics of the Nubia–Eurasia plate boundary zone. J Geophys 49:123–129

Vogt P, Jung W (2004) The Terceira Rift as hyper-slow, hotspot-dominated oblique spreading axis: a comparison with other slow-spreading plate boundaries. Earth Panet Sci Lett 218: 77–90

Ward SN (1998) On the consistency of earthquake moment rates, geological fault data, and space geodetic strain: the United States. Geophys J Int 134:172–186

Wilson M (1993) Plate-moving mechanisms: constraints and controversies. J Geol Soc 150:923–926

Yelles-Chaouch AK, Djellit H, Beldjoudi H, Bezzeghoud M, Buforn E (2004) The Ain Temouchent earthquake of December 22th, 1999. Pageoph 161(3):607–621

Ziegler PA (1993) Plate-moving mechanisms: their relative importance. J Geol Soc 150:927–940

Zittellini N, Gràcia E, Matias L, Terrinha P, Abreu MA, DeAlteriis G, Henriet JP, Dañobeitia JJ, Masson DG, Mulder T, Ramella R, Somoza L, Diez S (2009) The quest for the Africa–Eurasia plate boundary west of the Strait of Gibraltar. Earth Planet Sci Lett 280:13–50

Zoback ML (1992) First and second order patterns of stress in the lithosphere: the World Stress Map project. J Geophys Res 97: 11,703–11,728

Zoback ML et al (1989) Global patterns of tectonic stress. Nature 341:291–298